

## **PZT Preparation and Studying its Structural, Dielectric and Piezoelectric Properties**

**M.A.Batal, Fatima Sroujy, Sami Orfali\***

Department of Physics, College of Science, Aleppo University  
sami\_orfali@hotmail.com

---

**Abstract:** Crystalline nanostructured (PZT) with atomic ratio of the Pb:Zr:Ti of 1:0.53:0.47 was synthesized by a chemical method starting from Lead, Titanium and Zirconium salts and using low temperature synthesis path which supposed to compose a nanostructured PZT. Using XRF, a qualitative analysis had carried out to investigate that the samples contain Lead, Titanium and Zirconium. The samples were pressed as pellets then sintered at 1100°C. Using high voltage generator a poling process were achieved at (0.5 - 1.5) KV/mm at room temperature. Using AC measurements, a relative permittivity including real and imaginary parts in a function of frequency in the range (20 Hz-3 kHz) for unpoled samples at room temperature were measured in order to investigate the polarization processes. The relative permittivity and loss factor for poled samples were studied in a function of frequency where the poling process results in increasing the relative permittivity and decreasing the loss factor. The relative permittivity and loss factor were also studied in a function of temperature at fixed frequency. It's noticed that the relative permittivity increases with temperature up to many thousands times. Electromechanical factor, elastic compliance constants, and piezoelectric constant were calculated using Impedance spectra (IS) of the 1.5KV/mm poled sample.

**Keywords:** Piezoelectric, Poling process, Polarization, PZT, Piezoelectric parameters.

---

### **1 INTRODUCTION**

Lead ZirconateTitanate,  $Pb(Zr_xTi_{1-x})O_3$  (PZT) ceramics are an important class of piezoelectric, pyroelectric and ferroelectric materials.[1] Due to their excellent dielectric, piezoelectric and electro- optic properties, they find a variety of applications in high energy capacitors, non-volatile memories (FRAM), ultrasonic sensors, infrared detectors and electro optic devices[2-4]. PZT alloys belong to the family of ceramics, which are alloys of lead oxide, zirconium oxide, and titanium oxide ( $PbO$ ,  $ZrO_2$ , and  $TiO_2$ ). The familiar Perovskite structure appears in PZT alloys because there are equal numbers of divalent ( $Pb^{2+}$ ) and tetravalent ( $Zr^{4+}$  and  $Ti^{4+}$ ) cations. PZT alloys are in fact the alloys of two components:  $PbZrO_3$  and  $PbTiO_3$ . Thus, by controlling the composition and microstructure of the PZT alloys, it is possible to adapt their properties to suit particular applications [5]. The general chemical formula of our samples is  $PbZr_{1-x}Ti_xO_3$ , with  $x=0.47$ , due to the peculiarities of PZT is that, in the transition zone in between the two structures ( $x= 0.53$ ), called morphotropic phase boundary (MPB), which has high dielectric constants and piezoelectric coefficients [6]. Polycrystalline ferroelectric materials (ceramics) may be brought into a polar state by applying a strong electric field (10-100 kV/cm), usually at elevated temperatures. This process, called poling, can reorient domains within individual grains along those directions that are permissible by the crystal symmetry and that lie as close as possible to the direction of the field. A poled polycrystalline ferroelectric exhibits piezoelectric and pyroelectric properties, even if many domain walls are still present. After the removal of the poling field, a ferroelectric material possesses macroscopic polarization, called spontaneous polarization  $P_s$  [7,8]. The qualities of these piezoelectric materials are described in terms of some basic parameters such as piezoelectric, dielectric, elastic constants and electromechanical coupling factors. A number of methods, such as static and quasi-static, resonance and pulse-echo ultrasonic techniques [11,12] have been used to measure these constants. In the resonance method, some specific resonance modes may be excited by applying a variable frequency ac. field to piezoelectric samples of a specific shape, aspect ratio and specific polarization orientation. The resonance frequency  $f_r$  and anti-resonance frequency  $f_a$  corresponding to every sample can be recorded from the frequency spectrum. All physical parameters except dielectric constants, can be calculated from these resonance and anti-resonance frequencies according to the dynamic equations for these piezoelectric vibrators [13]. In this paper, chemical root is used to synthesize PZT at

low sintering temperature. XRF is used to detect the composition. High voltage source was used to pole the samples, Ac electrical measurements were used to study the electrical properties and piezoelectric properties including electromechanical coupling factor, compliance constants, and piezoelectric constant.

## 2 MATERIALS

Lead Nitrate ( $\text{PbNO}_3$ ), Titanium tetrachloride ( $\text{TiCl}_4$ ), Zirconium oxychloride octahydrate ( $\text{ZrOCl}_2 \cdot 8\text{H}_2\text{O}$ ), analytical grade, ammonia, ethylene glycol, distilled water, and Nitric acid, were used for chemical preparation.

## 3 EXPERIMENTAL

### 3.1 Preparation Of PZT

The Low-Temperature Synthesis path followed by auto-combustion process was adapted in this paper [2]. ( $\text{PbNO}_3$ ), ( $\text{TiCl}_4$ ), ( $\text{ZrOCl}_2 \cdot 8\text{H}_2\text{O}$ ), analytical grade, were used as starting materials. ( $\text{TiCl}_4$ ) and ( $\text{ZrOCl}_2 \cdot 8\text{H}_2\text{O}$ ) were solved in a distilled water at low temperature (about 20C) then a stoichiometric amount of ammonia was added to form a Precipitate of  $\text{TiO}(\text{OH})_2$  and  $\text{ZrO}(\text{OH})_2$ . Adding Nitric acid to the two solutions until the complete solution yielded  $\text{TiO}(\text{NO}_3)_2$  and  $\text{ZrO}(\text{NO}_3)_2$  solutions, then they added to the  $\text{Pb}(\text{NO}_3)_2$  solution with an appropriate amount of ethylene glycol which play two roles, one as a chelating agent and the other to provide the fuel for the auto combustion process. The atomic ratio of the Pb:Zr:Ti of solution was 1:0.53:0.47 with 2% excess of lead was introduced to compensate the evaporated amount during sintering process. After PZT precursor sol was obtained, the mixture was heated under 1000C until the gel formation. Then the gel was calcinated at 5000C. The formed powder was milled by a ceramic mortar, pressed under 5ton/cm<sup>2</sup> as disks of 10mm diameter and 1mm thickness. The sintering was at 11000C for 4h with temperature changes rate of 5oC/min. Then an XRF test was carried on the samples to investigate the compositional characterization. The disks were polished and washed by alcohol. In addition, an air-dry silver paste was applied to the samples surfaces as electrodes, to ensure a good electrical contact and introduce them for further characterization.

## 4 RESULTS AND DISCUSSIONS

### 4.1 Qualitative analysis

#### 4.1.1 XRF Measurements

Using XRF device, Unisantis® type Si-PIN with molybdenum (Mo) target operated at 50kV and 1mA, XRF spectrum was taken for the samples. Fig. 1 reveals the existence of the three elements (Lead, Zirconium and Titanium) in addition to toxic elements. Oxygen element was unable to be detected because it's out of the resolution of the device.

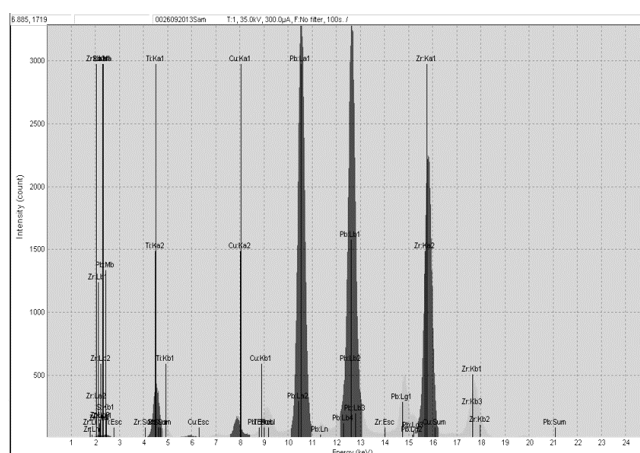


**Fig1.** XRF spectrum for PZT sample

#### 4.1.2 XRD measurements

To investigate the crystallization of prepared material treated at 1100°C, XRD spectrum was measured using APD 2000 PRO device from GNR Analytical Instrument Group®. Fig (2) shows XRD spectrum of the prepared material after compare it with JCPDS card File no.50-0346 [1], which reveals the formation of tetragonal Perovskite phase as well as Pyrochlore phase.

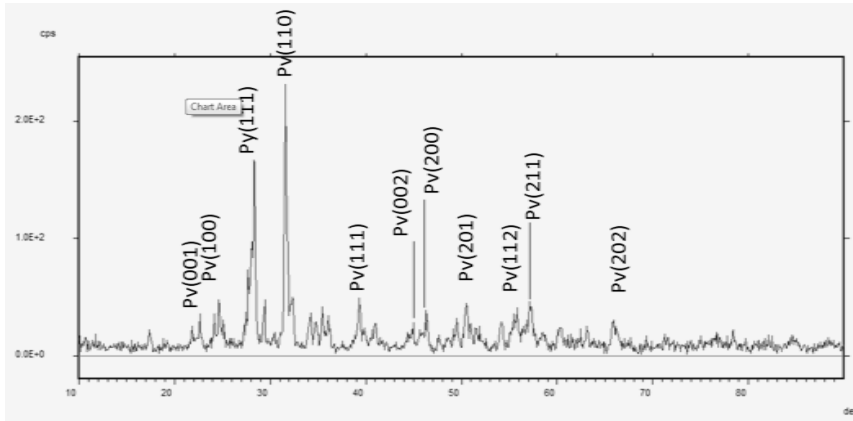


**Fig2.** XRD spectrum of the prepared material

Crystallization size was calculated using Scherrer Debye relation: [17]

$$D = \frac{K\lambda}{\beta \cos\theta}$$

Where  $K=0.94$  is the Scherrer constant,  $\lambda$  is the ray wavelength used for the diffraction.  $\beta$  Is the “full width at half maximum” of the sharp peak and  $\theta$  is the angle measured. The lattice strain was calculated by [16]:

$$\varepsilon = \frac{\beta \cos\theta}{4}$$

The lattice constant and crystallization size were used to calculate the dislocation density of the sample which can be defined as length of dislocation lines per volume unit of the sample by the expression:

$$\delta = \frac{15\varepsilon}{aD}$$

Table1. lists the crystallization size, lattice strain, and dislocation density of the sample calculated on the basis of (110) peak located at  $2\theta = 31.6^\circ$

**Table .1Crystallization size, lattice strain, and dislocation density of the sample.**

D(nm)	d(nm)	a(nm)	$\varepsilon \times 10^{-4}$ (lin <sup>-2</sup> .m <sup>-4</sup> )	$\delta \times 10^{14}$ (lin.m <sup>-2</sup> )
60.06	0.283	0.4002	5.86	3.659

## 4.2 Electrical Properties

### 4.2.1 Electrical Characterization for unpoled samples

The real and the imaginary parts of the relative permittivity and the loss factor  $\tan \delta$  were measured using LCR meter from MICROTTEST type 6379 in the range of frequency (20Hz-3 KHz) at room temperature. As shown in fig. 3, the real part of dielectric permittivity decreases sharply with increased frequency at range (20Hz-100Hz), then it decreases slightly at higher frequency.

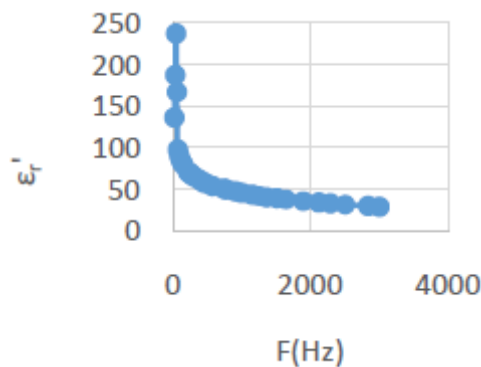


**Fig3.** Real part of relative permittivity in a function of frequency in the range of (20-3000 Hz) at room temperature.

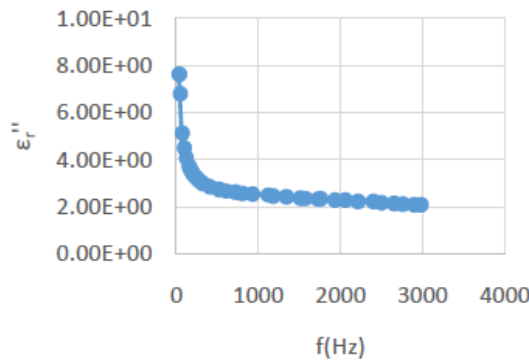


**Fig4.** The imaginary part of the relative permittivity in a function of frequency at room temperature.

Theoretically, this manner can be explained as following: At frequencies below 1 KHz. The four polarization mechanisms (electronic, ionic, orientational and space charge polarization) act. These polarizations involving the movements of charges either by orientation (i.e., orientational polarization) or through the migration of charge carriers (i.e., hopping or space charge polarization) belong to the relaxation regime. Because during the polarization or depolarization processes, a relaxation phenomenon occurs due to the time required for the charge carriers to overcome the inertia arising from the surrounding medium in order to proceed in their movement. Whereas at frequencies increases above 1 KHz, the only active polarization mechanisms polarizations associated with vibrations of electrons (i.e., electronic or optical polarization) or with vibrations of atoms or ions (i.e., atomic or ionic polarization). This behavior belongs to the resonance regime, because at certain frequencies a resonance will occur when the frequency of the excitation field is close to the natural frequency of the vibration or oscillation system. Where the real part of relative permittivity is theoretically given by Debye equation [9]:

$$\epsilon'_r = \epsilon'_{r\infty} + \frac{\epsilon'_{rs} + \epsilon'_{r\infty}}{1 + \omega^2\tau_0^2}$$

Where  $\epsilon'_{rs}$  and  $\epsilon'_{r\infty}$  are the low- and high-frequency values of  $\epsilon'_r$ , respectively.  $\tau_0$  Is the relaxation time. Fig. 4 shows the imaginary part of relative permittivity  $\epsilon''$  in function of frequency measured by LCR meter. It's similar to the relative permittivity variation with frequency

The values of  $\epsilon''$  decrease hundreds times before 1 KHz. That can explained by Koop's model which state that at low frequency, grain boundaries are responsible for the high resistivity, and charges need relatively high energy to hop between grains whereas at high frequency, grains are the responsible areas for conductivity and its resistivity is low [10]. So considering the hoping conductivity, the loss factor can be theoretically given by the following equation [9]:

$$\tan\delta = \frac{\omega\epsilon_0(\epsilon'_{rs} - \epsilon'_{r\infty})\omega\tau_0 + (1 + \omega^2\tau_0^2)\sigma}{\omega\epsilon_0(\epsilon'_{rs} + \epsilon'_{r\infty}\omega^2\tau_0^2)}$$

Where  $\sigma$  is the conductivity,

Fig5. Shows relative permittivity at different temperatures. It's clear that the curves have the same shapes at higher degrees which indicates that the same polarization process occur at temperatures below Curie point.

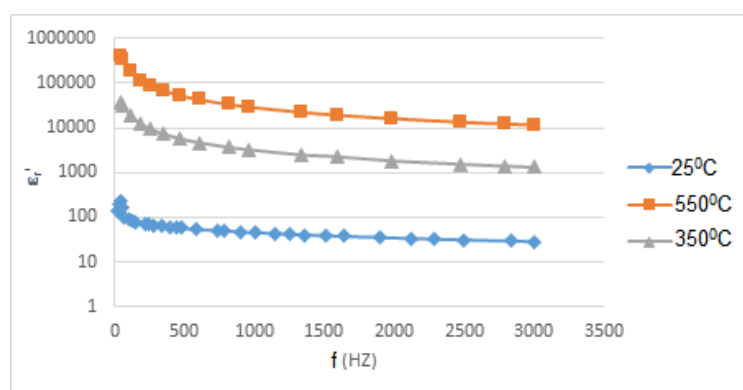


**Fig5.** Relative permittivity in a function of frequency at different temperature (25, 350, 550)<sup>o</sup>C

4.2.2 Poling the samples

For optimal poling, an electric field slightly higher than  $E_C$  (coercive field). Field should be applied at least for the switching time of the domains at room temperature [8]. A poled polycrystalline ferroelectric exhibits piezoelectric and pyroelectric properties, even if many domain walls are still present. After the removal of the poling field, a ferroelectric material possesses macroscopic polarization, called spontaneous polarization  $P_S$ . A small chamber was made to contain the sample. The chamber was made of Teflon and provided with terminals and thermocouple. As shown schematically in fig. 6.

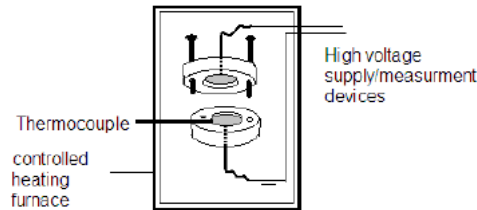


Fig 6. Schematic diagram for designed chamber.

Samples were submitted to an electrical field (1500V/mm, 1000V/mm and 500V/mm) under atmospheric conditions for half an hour.

4.2.3 Electrical Characterization for poled samples

After poling process application, relative permittivity and dielectric loss were measured. Fig. (7, 8). Represent the dielectric constant and dielectric loss factor as a function of frequency after poling with different poling electric fields.

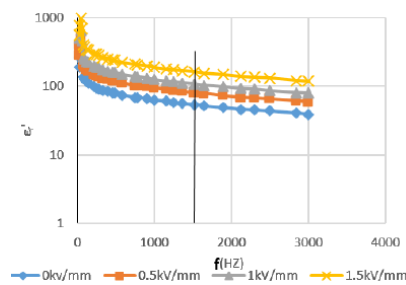


Fig7. Relative permittivity variations with frequency at different poling field

To illustrate the poling process effect on relative permittivity of material a vertical line is drawn at 1500Hz frequency, Table2. Lists the values of intersections points

Table2. Relative permittivity at certain values of poling field

Poling field(KV/mm)	0	0.5	1	1.5
Relative permittivity	54	81	108	162

Poled samples show significant enhancement of the relative permittivity with increasing the strength of the poling electric field.

Contrarily, the dielectric loss slightly decreased with increasing poling field especially at low frequencies. Table3. Lists the Intersection points of the vertical line drawn at 1000 Hz frequency. This can interpreted by the formation of domains walls due to the poling process which limits the conductivity resulting in decrease of the dielectric loss [18].

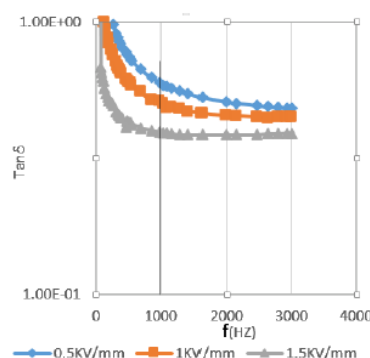


Fig8. Dielectric loss factor as a function of frequency after poling with different poling electric fields.

**Table3.** Dielectric loss at certain values of poling field.

Poling field(KV/mm)	0.5	1	1.5
Dielectric loss	0.596	0.513	0.394

**4.3 Piezoelectric measurements**

The electromechanical coupling coefficient is an important characteristic of piezoceramic elements used to measure the energy conversion efficiency. The dynamic electromechanical coupling coefficient proposed by Mason [9,14] can be computed by using the expression:

$$k_d^2 \approx \frac{f_a^2 - f_r^2}{f_r^2}$$

Where  $f_r$  is the resonant frequency and  $f_a$  is the antiresonant frequency. This coefficient is of special interest in designing piezoelectric elements. In order to determine the resonant frequencies of the material, Impedance spectra (IS) of the 1.5KV/mm poled sample was plot as shown in fig.9. From fig. 9:  $f_r=2.3625\text{MHz}$ ,  $f_a=2.35\text{MHz}$ .

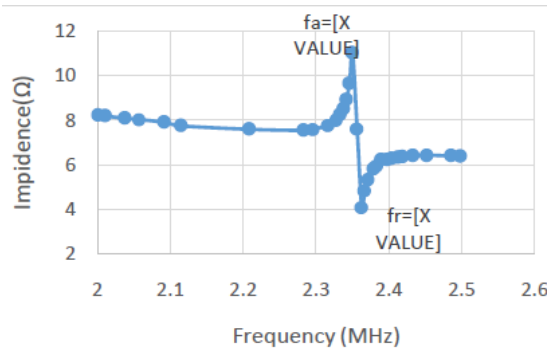


**Fig9.** Impedance spectrum for 1.5KV/mm poled sample with frequency range of [2-2.5MHz]

Once the resonant and the anti resonant frequencies have been determined, the elastic compliance at constant field  $y^E$  and at constant electrical displacement  $y^D$  can be calculated from relations [9, 15]:

$$f_R = \frac{1}{2l(\rho y^E)^{\frac{1}{2}}} \Rightarrow y^E = \frac{1}{4l^2 f_R^2 \rho}$$

$$f_A = \frac{1}{2l(\rho y^D)^{\frac{1}{2}}} \Rightarrow y^D = \frac{1}{4l^2 f_A^2 \rho}$$

Where  $\rho$  is the density of the specimen material and  $l$  is the length of the specimen. The superscript E in  $y^E$  means  $y$  value at constant field, signifying that the specimen is short-circuited, while the superscript D refers to  $y$  at constant displacement, signifying that the specimen is open-circuited.

Using the electromechanical factor, the piezoelectric constant  $d$  can be calculated from relation:

$$k^2 = \frac{d^2}{y\epsilon}$$

Where ‘ $\epsilon$ ’ is the permittivity, which can be determined from the capacitance measured at a frequency well below resonance, such as 3 kHz.

Using the previous relations and after estimation of density, resonant, antiresonant frequencies and permittivity at 3KHz frequency. Table (4) gives the calculate values of electromechanical factor, elastic compliance constants, and piezoelectric constant

**Table4.** Electromechanical factor, elastic compliance constants, and piezoelectric constant for the 1.5KV/mm poled sample.

$f_r$ (MHz)	$f_a$ (MHz)	$\rho$ (kg/m <sup>3</sup> )	$k$	$y^E$ (m <sup>2</sup> /N)	$y^D$ (m <sup>2</sup> /N)	$\epsilon$ (F/m)	$D$ (m/v)
2.3625	2.35	3603	0.4455	$5.95 \times 10^{-6}$	$7.43 \times 10^{-6}$	$1052.9 \times 10^{-12}$	$39.4 \times 10^{-9}$

As our sample is polycrystalline material and doesn't have a single spontaneous polarization axe, poling process created a spontaneous polarization along the poling electric field. Moreover, this developed evident piezoelectric properties.

## 5 CONCLUSIONS

Dielectric constant values decreases sharply with increased frequency in the range of (20KHz-100KHz), then the dielectric constant decreases slightly in the range of (1KHz-3KHz). Poling process increases the Dielectric constant of the samples until certain Poling voltage. Poling process decreases the dielectric loss of the material especially at frequencies below 1 KHz. Poling field (1.5 kV/mm) shows significant enhancement of the dielectric constant. Poling process makes evident piezoelectric properties along the poling electric field.

## REFERENCES

- [1] Haertling, G. H. 1999 - Ferroelectric ceramic. History and technology. J. Am. Ceram. Soc. 82, 797–818. Hu, T. and Desai, J.P. (2004) Soft-Tissue Material Properties under Large Deformation: Strain Rate Effect. Proceedings of the 26th Annual International Conference of the IEEE EMBS, San Francisco, 1-5 September 2004, 2758-2761.
- [2] Gajbhiye N. S.; Pandey P. K.; Smitha P. 2007 - **“Low-Temperature Synthesis of Nanostructured PZT for Dielectric Studies”** Synthesis and Reactivity in Inorganic, Metal-Organic, and Nano-Metal Chemistry, 37:431–435. Wit, E. and McClure, J. (2004) Statistics for Microarrays: Design, Analysis, and Inference. 5th Edition, John Wiley & Sons Ltd., Chichester.
- [3] Kim, K.; Lee, S. 2006 - **Integration of lead zirconium titanate thin films for high density ferroelectric random access memory**. J. Appl. Phys. 100, 51604–51611. Giambastiani, B.M.S. (2007) Evoluzione Idrologica ed Idrogeologica Della Pineta di san Vitale (Ravenna). Ph.D. Thesis, Bologna University, Bologna.
- [4] Yamashita, K.; Chansomphou, L.; Murakami, H.; Okuyama, M. 2004 - **Ultrasonic micro array sensors using piezoelectric thin films and resonant frequency tuning**. Sensors Actuators. 114, 147–153.
- [5] Noheda B.; Cox D. E.; Shirane G.; Gonzalo J. A.; Cross L. E.; Park S-E. 1999 - **A monoclinic ferroelectric phase in the Pb(Zr<sub>1-x</sub>Ti<sub>x</sub>) O<sub>3</sub> solid solution**, Appl. Phys. Lett. 74, 2059.
- [6] Dragan Damjanovic. 2006 - **Hysteresis in Piezoelectric and Ferroelectric Materials**. The Science of Hysteresis, Volume 3; I. Mayergoyz and G. Bertotti (Eds.); Elsevier.
- [7] Kamel T. M. 2007 - Poling and switching of pzt ceramics.
- [8] Kwan Chi Kao. 2004 - **Dielectric phenomena in solids**, book, ISBN 0-12-396561-6, Elsevier Academic Press, pp.-86-98.
- [9] Koops C. G. 1951 - Phys. Rev. 83 (121).
- [10] **IRE standards on piezoelectric crystals**, 1949, Proc. IRE, 37, PP.1378-1395, 1949.
- [11] **IRE standards on piezoelectric crystals-the piezoelectric vibrator: definitions and methods of measurement**, 1957”, Proc. IRE, 45, PP. 353-358, 1957.
- [12] Shining Zhu, BeiJiang .; Wenwu Cao. **Characterization of piezoelectric materials using ultrasonic and resonant Techniques”** SPIE Vol. 3341.
- [13] Mason W. P. 1950 - **Piezoelectric Crystals and Their Application to Ultrasonics**. New York: Van Nostrand.
- [14] Kuwata J.; Uchino K.; Nomura S. 1982 - Jpn. J. Appl. Phys. 21, 1298. **[IEEE Standard on piezoelectricity**. ANSI/IEEE Std. 176-1987.
- [15] N J SUTHAN KISSINGER, M JAYACHANDRAN, K PERUMAL and C SANJEEVI RAJA, **“547 Structural and optical properties of electron beam evaporated CdSe thin films”** Bull. Mater. Sci, Vol. 30, No. 6, December 2007, pp. 547-551. Indian Academy of Sciences.
- [16] B.M. Oliver, J.M. Cage, **Electronic measurement and Instrumentation**, McGraw- Hill, New York 1971.
- [17] J Erhat, Satoshi Wada, **“Theoretical calculation of the resonant frequency temperature dependence for domain-engineered piezoelectric resonators”**. Materials Science and Engineering B 120 (2005) 175-180.